

Dear Author,

Please, note that changes made to the HTML content will be added to the article before publication, but are not reflected in this PDF.

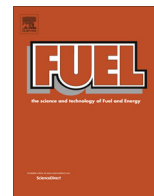
Note also that this file should not be used for submitting corrections.



Contents lists available at ScienceDirect

Fuel

journal homepage: www.elsevier.com/locate/fuel



On-line analysis of organic emissions from residential wood combustion with single-photon ionisation time-of-flight mass spectrometry (SPI-TOFMS)

H. Czech^a, O. Sippula^{b,c}, M. Kortelainen^b, J. Tissari^b, C. Radischat^{a,c}, J. Passig^{a,c}, T. Streibel^{a,c,d,*}, J. Jokiniemi^{b,c}, R. Zimmermann^{a,c,d}

^aJoint Mass Spectrometry Centre, Chair of Analytical Chemistry, Institute of Chemistry, University of Rostock, 18059 Rostock, Germany

^bFine Particle and Aerosol Technology Laboratory, Department of Environmental Science, University of Eastern Finland, P.O. Box 1627, FIN-70211 Kuopio, Finland

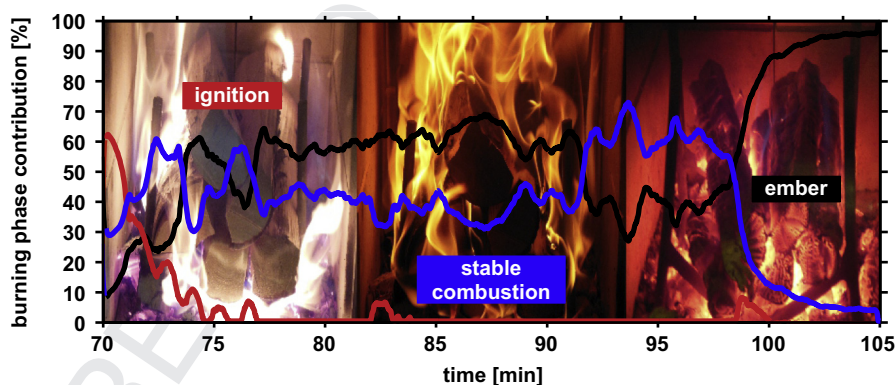
^cHelmholtz Virtual Institute of Complex Molecular Systems in Environmental Health (HICE), Germany¹

^dJoint Mass Spectrometry Centre, Cooperation Group "Comprehensive Molecular Analytics", Institute of Ecological Chemistry, Helmholtz Zentrum München – German Research Centre for Environmental Health, 85764 Neuherberg, Germany

HIGHLIGHTS

- Examination of VOC, IVOC and SVOC emission from masonry heater with air staging.
- High time resolution allows to monitor short combustion events.
- Semi-quantification of VOC and IVOC for three common firewoods.
- Highest organic emissions in first two of six batches.
- Molecular signature of gas phase for each burning phase.

GRAPHICAL ABSTRACT



ARTICLE INFO

Article history:

Received 4 June 2015
Received in revised form 9 March 2016
Accepted 10 March 2016
Available online xxx

Keywords:

Masonry heater
VOC
Air staging
Batch combustion
Burning phase

ABSTRACT

A study about the temporal variation of organic emissions from a modern wood log fired masonry heater was carried out with different gas analysis techniques: single-photon ionisation time-of-flight mass spectrometry (SPI-TOFMS) for real-time analysis of volatile (VOC), intermediate-volatile (IVOC) and semi-volatile organic compounds (SVOC), and a gas analyser system for gaseous components CO₂, CO, NO_x and organic gaseous carbon (OGC, quantified by flame ionisation detector). The emissions of three in Europe common types of firewood (beech, birch and spruce) were investigated by combustion of six consecutive batches of 2.5 kg each over 4 h. Batchwise emissions and temporal variations during combustion were discussed. Emission factors over the whole combustion cycle for OGC, VOC and IVOC were right up to one order of magnitude lower than in many previous studies due to latest improvements of air staging technology in wood log fired masonry heaters, whereas CO and NO_x remained comparable. Regarding each combustion experiment, more than 50% of the total intensity of the mass spectra occurred during the combustion of the first two batches. Moreover, the molecular signatures of burning phases ('ignition', 'stable combustion' and 'ember') were examined by using non-negative matrix factorisation (NMF) and

* Corresponding author at: Joint Mass Spectrometry Centre, Chair of Analytical Chemistry, Institute of Chemistry, University of Rostock, 18059 Rostock, Germany. Tel.: +49 381 498 6536; fax: +49 381 498 118 6527.

E-mail address: thorsten.streibel@uni-rostock.de (T. Streibel).

¹ www.hice-vi.eu.

principal component analysis (PCA) in sequence. Marker substances for wood or biomass combustion, such as phenolic species or furan derivatives, exhibited highest relative abundance during 'stable combustion', whereas 'ember' is distinctly characterised by polyunsaturated hydrocarbons, such as benzene or naphthalene, through pyrosynthesis; in 'ignition', secondary decomposition products dominated. Nevertheless, highest quantitative emissions always occurred during 'ignition' at the beginning of each batch, followed by the phases 'ember' and 'stable combustion'.

© 2016 Published by Elsevier Ltd.

1. Introduction

According to Directive 2009/28/EC, the Commission of the European Union fixed targets for its member states to reach a mean percentage of 20% renewable energy of the final energy consumption in the whole European Union until 2020. The directive was preceded by the decision to pursue an incorporative energy and climate policy, declared in the European climate package from 2007. A potential way to produce energy from renewable source is the combustion of wood. In 2010, wood amounted for 38%, 50% and 30% of renewable energy consumption in the three most heavily populated EU countries Germany, France and United Kingdom [1]. Previous studies has been shown that wood combustion contributes significantly to indoor and outdoor air pollution, especially to ambient air fine particle concentrations [2–4], known for inducing adverse health effects [5–7]. In addition to particulate emissions, wood combustion is also a significant source of volatile organic compound (VOC) emissions which are known for their deleterious effect on human health and as precursors for atmospheric secondary organic aerosol formation [8–10]. With ongoing improvements on wood stoves, the composition of released VOC might change qualitatively as well as quantitatively and has to be evaluated consistently to support toxicological studies and to keep atmospheric models updated.

Most of previous studies about wood combustion-related VOC used adsorbents [4,11–13] or gas sampling bags [14] for thermal-desorption gas-chromatography (TD-GC) to obtain integrated results of one combustion experiment. However, these techniques are time consuming and cannot gather the dynamics of wood combustion. Thus, time-resolved information was predominantly achieved by Fourier-transform infra-red spectroscopy (FTIR), proton-transfer-reaction mass spectrometry (PTR-MS), or resonance-enhanced multiphoton ionisation time-of-flight mass spectrometry (REMPI-TOFMS) [15–21]. Moreover, pyrolysis of small amounts of wood with evolved gas analysis was carried out to examine volatile decomposition products of wood or its major polymeric components lignin, cellulose and hemicellulose [22–24].

This following study was carried out in the framework of the Helmholtz Virtual Institute of Complex Molecular Systems in Environmental Health (HICE) at the University of Eastern Finland (UEF). The project HICE investigates causes and mechanisms of environmentally influenced diseases for a deeper understanding of impacts of anthropogenic aerosols, such as wood combustion aerosols, on human health. Innovative in-vitro human lung tissue models were exposed to these aerosols. State-of-the-art analytical techniques are applied for comprehensive, non-targeted analyses of small molecules in anthropogenic aerosols and on different biological levels (transcriptome, proteome, metabolome, toxicological parameters).

As a part of the chemical analysis in HICE, we describe on-line measurements with single-photon ionisation time-of-flight mass spectrometry (SPI-TOFMS) to characterise VOC, intermediate-volatile (IVOC) and semi volatile organic compounds (SVOC) from a modern masonry heater, which was equipped with the novel

technique of air staging [25] and fuelled with three types of commonly used firewood (beech, birch and spruce). The potential of SPI-TOFMS to examine and monitor short-term events in combustion/pyrolysis experiments with low detection limits, in particular of wood combustion [26], has been previously demonstrated [27,28]. Due to a different selectivity to PTR-MS and low fragmentation rates, SPI-TOFMS augments the knowledge from previous studies in that field and enables to unravel the molecular composition of wood combustion-derived VOC to SVOC.

In the following, batch-to-batch emission factors (EF) of CO, NO_x, OGC and 10 selected VOC/IVOC are presented and compared with EF from stoves of previous studies. Finally, the high time resolution is used to figure out consequences of occasionally inappropriate ignition and qualitative differences of emission in three burning phases by applying non-negative matrix factorisation (NMF).

2. Materials and method

2.1. Experimental setup

2.1.1. Stove setup

The combustion experiments were performed with a modern masonry heater (Hiisi 4; Tulikivi Ltd., Finland) which was equipped with an upright enclosed firebox, double glass window door and controlled combustion air supply. In general, the combustion process is relatively fast and combustion chamber temperatures are relatively high in this type of heat-retaining fireplaces. The heat released during the combustion process is retained in the surrounding massive soapstone structure and released slowly as supplemental heat.

Flue gases were led from the firebox to the upper combustion chamber and then downwards through side ducts into the stack. The stack was placed below a hood, and draught was regulated with two dampers. The target value for the pressure in the stack was (12.0 ± 0.5) Pa below ambient pressure.

The combustion air was distributed as primary air flow through the grate (less than 20% of total air supply), as secondary air flow above the fuel batch through small rifts in the firebox (about 45%) and as window flushing air (about 35%). The advantages of this type of air staging in batch combustion appliances are reduced gaseous and particulate organic emissions compared to conventional non-staged combustion [25,29].

2.1.2. Fuel characterisation

Two hardwoods (beech, birch) and one softwood (spruce), which are widespread as fuel for residential heating, were tested. Analysis of the wood concerning calorific properties, water content and elemental composition was conducted by an external laboratory based upon international standards (Table 1).

2.1.3. Combustion procedure

In total, eight combustion experiments were carried out including two beech ('beech1' and 'beech2'), four birch ('birch1', 'birch2', 'birch3' and 'birch4') and two spruce experiments ('spruce1' and

Table 1
Elemental composition and properties of the log woods.

Property	Unit ^a	Method	Birch	Beech	Spruce
Moisture	%	DIN EN 14774-2	7.2	9.0	7.4
Ash at 550 °C	% (w/w)	DIN EN 14775	0.69	1.3	0.58
Carbon	% (w/w)	DIN EN 15104	51.0	50.3	52.0
Hydrogen	% (w/w)	DIN EN 15104	6.0	5.8	5.9
Nitrogen	% (w/w)	DIN EN 15104	0.40	0.36	0.36
Oxygen	% (w/w)	Calculated	41.9	42.3	41.1
Sulphur	% (w/w)	DIN EN 15289	0.006	0.037	0.009
Chlorine	% (w/w)	DIN EN 15289	<0.005	<0.005	0.005
Potassium	mg/kg	DIN EN ISO 17294-2	500	1330	640
Lower heat value	kJ/kg	DIN EN 14918	18140	17,790	18,640

^a Related to dry basis.

'spruce2'). Due to an intermittent shutdown of the gas analyser system, experiment 'birch3' was excluded from EF calculations. Each experiment lasted for four hours, during which six batches of wood were burned. In the first batch, ten logs were laid cross wise (0.23 kg each). On top of the logs 150 g of smaller wood pieces were placed as kindling. Ignition of the first batch was always done from the top by a basic lighter fuelled with butane. Batches 2–6 consisted of five logs (0.5 ± 0.05) kg each. The weight of each batch was (2.50 ± 0.20) kg, so in each experiment the total amount of wood was 15.0 kg.

Apart from the duration of the first batch the combustion procedure was consistent for all wood species. For 'beech2' and each birch experiment, the first batch lasted for 30 minutes because of faster burning, while for 'spruce1', 'spruce2' and 'beech1' the duration was 35 min. In all cases batches 2 to 6 were burned for 35 min and after batch 6 no more wood was refilled. The remaining ember was stoked and the secondary air channels were closed according to the official instructions given by the stove manufacturer. The embers went on glowing until a total time of four hours was reached (35 min with 'beech2' and birch, 30 min with spruce and 'beech1'). As combustion experiments were done in consecutive days, the cooling of the combustion appliance was enhanced with a blower between the experiments, in order to cool the stove down to room temperature.

2.2. Instrumentation

2.2.1. Bulk gas and temperature analysis

Flue gas composition including carbon monoxide (CO), carbon dioxide (CO₂), oxygen (O₂) and nitrogen oxides (NO_x) were measured continuously by a gas analyser system (ABB, Cemas). The sum emissions of organic gaseous compounds (OGC) were quantified by a flame ionisation detector (ABB, Multi-FID 14), which was calibrated against propane. All gaseous emissions were measured directly from undiluted stack gas through an insulated and externally heated (180 °C) sampling line. Flue gas temperature was determined from the stack right after the masonry heater gas outlet with a K-type thermocouple.

2.2.2. Single photoionisation time-of-flight mass spectrometry (SPI-TOFMS)

VOC, IVOC and SVOC of the emission were analysed by a time-of-flight mass spectrometer (TOFMS; Compact Reflectron Time-of-Flight Spectrometer II, Kaesdorf Geräte für Forschung und Industrie) with single-photon ionisation (SPI) at 118 nm (photon energy of 10.49 eV). SPI refers to a soft ionisation technique, thus leading to molecular ions and low fragmentation. Every compound with an ionisation energy below the photon energy becomes ionised whereby the ionisation efficiency strongly depends on the compound class [30]. VUV-photons of 118 nm were generated by multiple frequency increases of the fundamental radiation of

1064 nm of a Nd:YAG-laser (Spitlight 400, Innolas GmbH, Krailling, Germany). During the experiments, D₃-toluene (mass-to-charge ratio *m/z* = 95; toluene methyl-D₃, 98% purity, Cambridge Isotope Laboratories, Inc.) was constantly added as internal standard leading to a concentration of 0.911 ml/m³ (=0.911 ppmv) in the raw gas. The following mass spectra were related to the intensity of *m/z* 95, which represents 0.806 ppmv due to its isotopic composition and a small yield of the tropylium ions. The flue gas was sampled at 220 °C with stepwise increasing temperature to 245 °C to prevent condensation. At 230 °C a glass fibre filter, which was replaced before every new combustion experiment, was installed to hold back particles and to approximate an atmospheric gas-particle partitioning of SVOC. For a more detailed description of the instrumental setup see also supplemental material S1.

2.3. Non-negative matrix factorisation (NMF)

Positive or non-negative matrix factorisation (PMF/NMF) can be used to combine measured variables according to their abundances in the experiment to identify single processes, e.g. to determine burning phases in batchwise wood combustion [20]. NMF is an iterative technique and partitions a non-negative *n*-by-*m* matrix *M* in to a *n*-by-*k* matrix *W* and a *k*-by-*m* matrix *H*. The number of factors *k* is the only predefined variable. *W* and *H* are computed by an alternating least-squares algorithm to minimise the functional

$$f(W, H) = \frac{1}{2} \|M - WH\|_F^2 \quad (1)$$

where $\|X\|_F$ computes the Frobenius-norm of a non-negative matrix *X*:

$$\|X\|_F = \sqrt{\text{trace}(X^T \cdot X)} \quad (2)$$

Thus the product of *W* and *H* is called a non-negative factorisation of *M*, although *WH* has not to be equal to *M*. NMF requires no further input variables than *k*, so the iteration starts with random initial values *W*₀ and *H*₀ for *W* and *H*, respectively. To avoid convergence into a local minima, *W*₀ and *H*₀ are optimised before running the NMF by using a multiplicative algorithm, which is more sensitive towards the convergence criterion [31].

Many studies in atmospheric science refer to the algorithm by Paatero and Tapper named positive matrix factorisation (PMF) [32], but PMF and NMF can be regarded as interchangeable [31].

3. Results and discussion

3.1. Emissions of 4 h combustion cycle

The masonry heater emitted approximately one order of magnitude lower concentrations of VOC than combustion appliances in

Table 2
EF of OGC, CO, NO_x in mg/MJ and 10 single VOC and IVOC in µg/MJ (dry basis).

	OGC	CO	NO _x	PRP	AA	VAC	BTD	BENZ	TOL	STYR	IND	NAP	MNAP
beech1	27.7	1496	106.0	1568.3	3889.8	95.6	275.4	1607.6	202.4	78.7	50.6	326.0	22.5
beech2	22.4	1372	117.6	1068.0	2563.2	61.8	179.9	1096.1	123.7	50.6	33.7	213.6	11.2
birch1	13.4	2152	106.1	788.3	1075.0	33.1	170.9	909.6	115.8	44.1	27.6	215.0	22.1
birch2	18.7	1602	104.5	529.2	804.9	38.6	198.5	766.3	148.8	55.1	22.1	176.4	22.1
birch4	15	1153	104.7	622.9	1405.7	44.1	198.5	766.3	137.8	55.1	27.6	176.4	33.1
spruce1	44.9	1291	83.1	4662.0	8632.0	305.8	1078.3	2376.6	777.9	203.9	166.3	627.7	91.2
spruce2	19.6	1663	86.9	1073.0	2832.6	85.8	295.1	1201.7	236.1	69.7	32.2	279.0	26.8

PRP = propene; AA = acetaldehyde; VAC = vinylacetylene; BTD = butadiene; BENZ = benzene; TOL = toluene; STYR = styrene; IND = indene; NAP = naphthalene; MNAP = methyl naphthalene.

previous studies without air staging, while emissions of CO and NO_x were not affected (Table 2).

In our experiments, CO levels cover a range from 20 g/kg ('birch4') to 38 g/kg ('birch1'). NO_x concentrations were almost constant in all experiments, viz. 1.5 g/kg ('spruce1' and 'spruce2')–2.1 g/kg ('beech2'), and lie within the range of literature data. OGC refers to a quantity which represents the sum of volatile organic compounds and varies the most by a factor of three, from 0.23 g/kg ('birch1') to 0.79 g/kg ('spruce1'). OGC results of this study agree well with data from Lamberg et al. [33] and Tissari et al. [34], who both burned birch wood in a modern masonry heater with improved secondary air supply. Lower emissions of OGC compared to results from Nuutinen et al. [25], who used a similar modern masonry heater with air staging, can be explained by the longer experiment time in our study during which the combustion chamber temperature increased and OGC declined (Table S2). Regarding the different types of wood, birch wood features the lowest emission of OGC, but the limited number of experiments does not allow generalising this result.

By using SPI-TOFMS together with an internal standard, semi-quantification of single compounds is principally possible (supplemental material S3.2.). The EF of VOC and IVOC follow the same trend as OGC from this study and are also one order of magnitude lower than concentrations from previous studies [11,13,25,35]. For example, propene, which is one of the most abundant compounds, is determined as 9.6–14.3 mg/kg for birch wood, whereas Tissari et al. [35] measured even 210 mg/kg wood (Table S3).

3.2. Time-resolved emission

3.2.1. Emission of single wood batches

Batchwise emissions were compared by averaging measured quantities (OGC, CO, NO_x and intensities of *m/z*) over each batch including the char-burning phase at the end and calculating their proportion to the overall emission (Fig. 1); batchwise EF can be found in the supplemental material (Table S4). The highest peak intensities can be observed during the first two batches, whereas from the third batch down to char-burning the intensity of most *m/z* decreases steadily. Thus, the number of batches affects the integrated emission of one batch combustion experiment. For example, the combustion procedure of Nuutinen et al. [25] included only three batches and no char-burning, leading to higher emission factors for OGC. The combustion of remaining char at the end of the experiment reveals the smallest fraction of the overall organic emission.

To find out which measured concentrations are significantly higher in one batch or two batches when compared to the whole 4 h combustion cycle, a single and double Grubbs' Outlier Test [36] for six batches (excluding char-burning) were performed. It turned out that mathematical outliers are maxima and mainly occur in the first two batches. In six of seven experiments, CO was released in significantly higher concentrations than in other batches. Nevertheless, CO emissions occur for 30–70% during the

last 30 min in the char-burning phase when considering the whole combustion cycle. By contrast, NO_x emissions were more comparable from batch to batch and much lower during char-burning. Apart from 'birch1' and 'birch2', OGC emissions were always significantly enhanced in the first two batches, but not for every detected VOC, IVOC or SVOC. In five of the eight experiments, *m/z* 40 (allene, propyne), 66 (cyclopentadiene), 78 (benzene), 92 (toluene), 94 (phenol), 128 (naphthalene), 118 (indane), 104 (styrene), 102 (phenylacetylene), 168 (dibenzofuran, methylsyringol), 178 (phenanthrene, anthracene), 180 (vinyl-syringol, coniferyl alcohol, fluorenone) and 202 (pyrene/fluoranthene) are significantly more abundant in the first two batches. Except coniferyl alcohol and methylsyringol, each one of these compounds does not belong to the group of wood-specific emissions and are more general combustion products. The absence of oxygen in the molecules or low O/C ratio as well as low H/C ratio indicate secondary formation by pyrolysis of precursors such as phenolic species [37,38], or by pyrosynthesis in flames [39,40].

One of the most abundant hydrocarbons is benzene, which is released with a proportion of 51–63% of the whole emission only during the first batch. Many studies about the pyrolysis of pure cellulose/hemicellulose, and lignin or lignin monomers by thermal analysis are available, but none of them observed a considerable release of benzene below 900 K [24,38,41]. Therefore, high benzene emissions during first batches are likely caused by pyrosynthesis, although the temperature inside the combustion chamber is the lowest during the whole combustion procedure. Additionally, this hypothesis is supported by the temporal trend of the smallest PAH naphthalene (*m/z* 128), which is also formed by pyrosynthesis [42] and runs proportionally with benzene in all batches of all experiments (correlation coefficient *r* = 0.98). Moreover, the two VOC toluene and benzene play an important role for atmospheric scientists: Their ratio toluene-to-benzene (tol/benz) can be used as photochemical clock due to higher reaction rates of toluene with OH-radicals compared to benzene as well as for source apportionment studies. Jordan et al. state that tol/benz is lower than 1 for biomass burning in residential areas [43], but for the examined stove with air staging this limit seems too rough since tol/benz of all batches and wood types show a mean ratio of 0.17 (median: 0.15; 1st quartile: 0.10; 3rd quartile: 0.22). This fact might become more relevant when prospective atmospheric studies of source apportionment are conducted in residential areas of developed countries.

Three of four birch experiments show significantly enhanced intensities of several *m/z* in the third batch compared to the 4 h combustion experiment. One explanation for significantly elevated intensities in the third batch might be that the combustion residue from the previously burned logs is lower than for other woods. Consequently, there might be not enough combustion residues to ignite the new logs efficiently so that the emission profile is more comparable to the first batch. Moreover, experiment 'spruce1' attracts special attention because the first batch account for approximately 70% of the total intensity. 'Spruce1' is compared

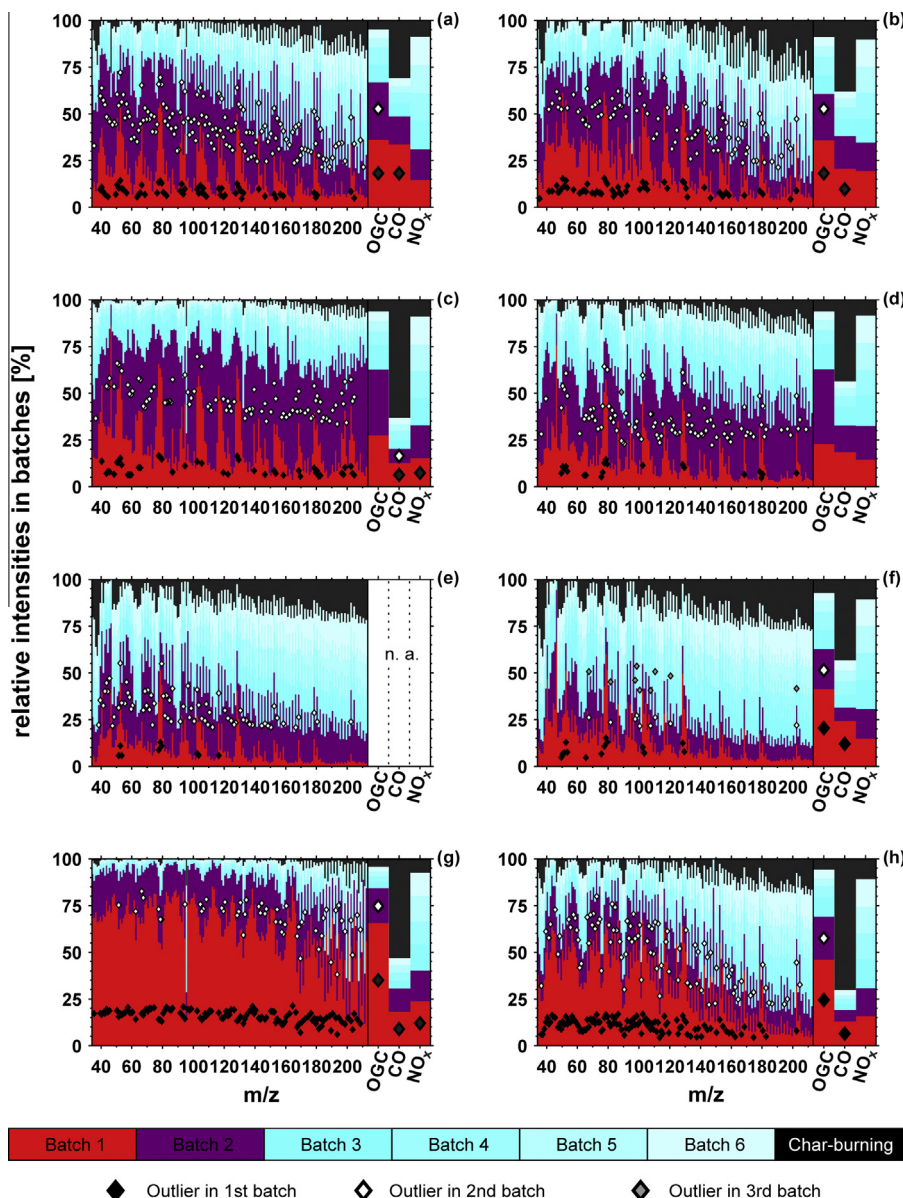


Fig. 1. Proportions of m/z -intensities, OGC, CO and NO_x in batches and char-burning phase for (a) 'beech1', (b) 'beech2', (c) 'birch1', (d) 'birch2', (e) 'birch3', (f) 'birch4', (g) 'spruce1', and (h) 'spruce2'. For single and double Grubbs' Outlier Test, only batches one to six, but no char-burning were considered. Significantly enhanced intensities are marked with diamonds in black, white and grey for batch numbers one, two and three, respectively.

374 to the second spruce experiment 'spruce2' and discussed more in detail in the following Section 3.2.2.
375

376 3.2.2. Proper vs. interrupted ignition

377 SPI-TOFMS provides on-line combustion monitoring with temporal resolution of 1 s. Together with flue gas temperature, CO,
378 NO_x and OGC, this benefit can be used to analyse temporal variations of the combustion process and to examine the differences
379 between the experiments 'spruce1' and 'spruce2' (Fig. 2).
380

381 First of all, the peaks of organic compounds during the first minute of the first batch can be assigned to the combustion of the fast-
382 burning kindlings utilised to ignite the whole batch. Regarding the flue gas temperature of both experiments, it is striking that their
383 trends show different behaviour. For the temperature in 'spruce2' (Fig. 2b), the typical bell-shaped curve [35] can be observed, which
384 is linked to combustion phases [20]. At the beginning, the flue gas temperature rises when the logs are ignited, followed by peaking
385 during harsh and stable combustion and finally resulting in a slight
386 decline. On the contrary, in experiment 'spruce1' the temperature drops between 5 min and 8.5 min before rebounding (Fig. 2a). In
387 this time, OGC and CO grow dramatically, while CO_2 decreases, which all indicate incomplete combustion. The same observation
388 can be made to a lower extent between 18 min and 23 min when the flue gas temperature twice reaches a plateau. However,
389 increased concentration of OGC is not defrayed in equal proportions of all organics, which can be monitored by benzene (m/z
390 78, pyrosynthesis), guaiacol (m/z 124, lignin-monomer), coniferyl alcohol (m/z 180, lignin-monomer of soft wood) and levoglucose
391 none/hydroxymethylfurfural (m/z 126, both decomposition products of (hemi-)cellulose) in Fig. 2c. When the flue gas temperature
392 drops, a smouldering-like phase begins with a disproportional increase in primary decomposition from lignin and carbohydrates.
393 The ratios of the peak intensities of the three primary decomposition products to benzene grow from 5 min on and spike between
394 18 min and 23 min. It seems that the combustion progress is disturbed and releases intensified primary decomposition products.
395
396
397
398
399
400
401
402
403
404
405
406
407
408

391 decline. On the contrary, in experiment 'spruce1' the temperature drops between 5 min and 8.5 min before rebounding (Fig. 2a). In
392 this time, OGC and CO grow dramatically, while CO_2 decreases, which all indicate incomplete combustion. The same observation
393 can be made to a lower extent between 18 min and 23 min when the flue gas temperature twice reaches a plateau. However,
394 increased concentration of OGC is not defrayed in equal proportions of all organics, which can be monitored by benzene (m/z
395 78, pyrosynthesis), guaiacol (m/z 124, lignin-monomer), coniferyl alcohol (m/z 180, lignin-monomer of soft wood) and levoglucose
396 none/hydroxymethylfurfural (m/z 126, both decomposition products of (hemi-)cellulose) in Fig. 2c. When the flue gas temperature
397 drops, a smouldering-like phase begins with a disproportional increase in primary decomposition from lignin and carbohydrates.
398 The ratios of the peak intensities of the three primary decomposition products to benzene grow from 5 min on and spike between
399 18 min and 23 min. It seems that the combustion progress is disturbed and releases intensified primary decomposition products.
400
401
402
403
404
405
406
407
408

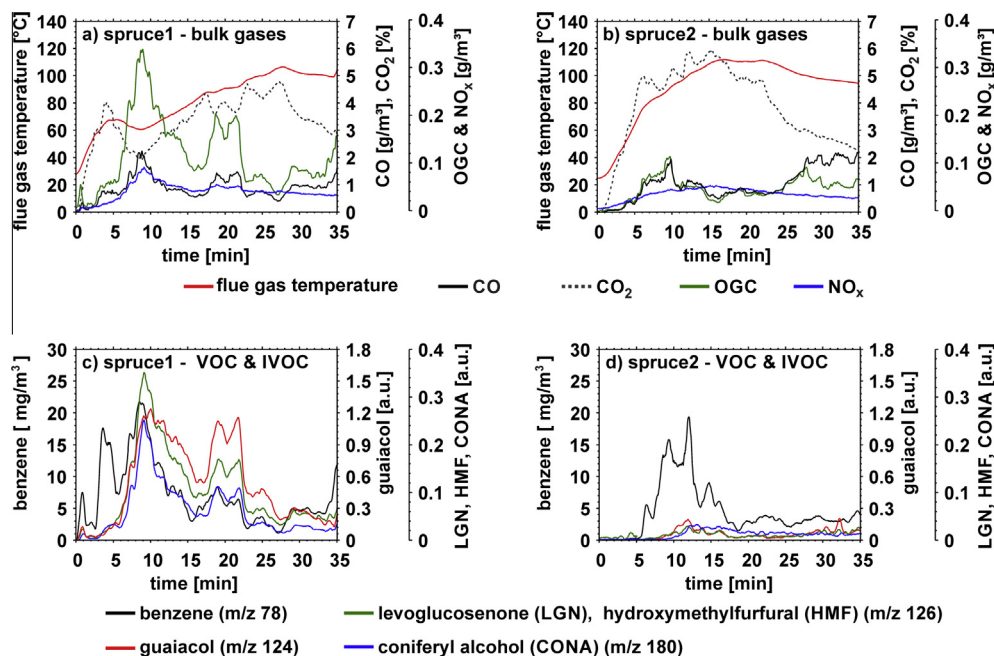


Fig. 2. First batch temporal trends of experiments 'spruce1' (left) and 'spruce2' (right) for most abundant gaseous emission (top), and VOC/IVOC (bottom).

409 Comparing the first batch of 'spruce1' and 'spruce2', benzene is
410 only enhanced 1.6-fold, whereas *m/z* of guaiacol, levoglucose
411 none/hydroxymethylfurfural and coniferyl alcohol are 10-fold, 26-
412 fold and 5-fold increased. OGC, which represents all VOC and IVOC,
413 is only 2.5-fold increased. Moreover, the failed ignition of the first
414 batch affects the results of the whole combustion experiment, elu-
415 cidated by highest emission factors for OGC and all semi-quantified
416 components. Only minor elevation is observed for NO_x during the
417 temperature drop compared to other experiments. Experiment
418 'spruce1' is the only one where such a smouldering phase during
419 ignition obviously occurred.

3.2.3. Determination of burning phases and their molecular signature

420 The wood combustion passes through different burning phases,
421 thus the emission profile even changes distinctly with time during
422 one batch and even covers a dynamic range up to four orders of
423 magnitude. Each *m/z* features its highest abundance at the begin-
424 ning of each batch, while the intensity maxima tend to decrease
425 with ongoing batches. Within one single batch, two different tem-
426 poral trends for *m/z* traces are perceived: The first group of *m/z*
427 diminish steadily, whereas the second group has its maximum at
428 the beginning as well, but passes through a minimum and
429 increases again towards the end of the batch. Mainly *m/z* of 78
430 (benzene), 128 (naphthalene), 54 (butadiene), 52 (vinylacetylene),
431 and 42 (propene) belong to the second group, remaining *m/z* to the
432 first group, which indicates that the combustion passes through
433 different phases.
434

435 Additional to the particulate phase analysed by aerosol mass
436 spectrometry [20], wood combustion burning phases can also be
437 determined by the gas phase through SPI mass spectra and subse-
438 quent NMF. Only even *m/z* were selected to diminish the original
439 data because wood consists mainly of carbon, hydrogen and oxy-
440 gen, which can only form molecules of even masses and thus
441 even-numbered molecular ions. For NMF, a three factor solution
442 was preset to obtain results analogue to PMF results by Elsasser
443 et al. [20].
444

445 From NMF, two matrices were obtained: the first one represents
446 the absolute factor contribution, the second set contains the factor
447 loadings. Burning phases 'ignition', 'stable combustion' and 'ember'

447 were identified by their temporal trends, previous burning phase
448 identification by OGC, CO₂ and CO can be found in the [supplemen-
449 tal material S5.1](#). The relative factor contributions and factor load-
450 ings for 'spruce2' in% were calculated and exemplarily illustrated
451 in Fig. 3a and b. So far, the contribution of single organic com-
452 pounds to these phases has not been investigated yet. On that
453 account, molecular patterns of each burning phase were figured
454 out from 24 obtained factor loadings by principal component anal-
455 ysis (PCA) [44]. Before starting the PCA based upon covariance,
456 NMF factor loadings were normalised to their respective total
457 intensity and subsequently centred.

458 The first two principal components (PC1 and PC2) explain 82.7%
459 and 10.9% of the total variance. In the score plot, burning phases
460 are well separated on the positive x-axis (ember) and in the second
461 (stable combustion) and third quadrant (ignition). However, clus-
462 tering of wood types cannot be observed, therefore the burning
463 conditions, e.g. a proper ignition, seems to be more important for
464 the examined combustion appliance.

465 In positive direction PC1 is exclusively loaded with *m/z* corre-
466 sponding to unsaturated hydrocarbons, e.g. benzene (*m/z* 78),
467 naphthalene (*m/z* 128), vinylacetylene (*m/z* 52) and allene/propyne
468 (*m/z* 40), which are mainly formed by pyrosynthesis. Thus, the pos-
469 itive loading of PC1 can be regarded as a convenient representative
470 for the glowing of charcoal-like combustion residues.

471 Compared to 'ember', 'ignition' and 'stable combustion' are only
472 separated by PC2. The positive loading of PC2 can be predomi-
473 nantly assigned to C2- to C5-carbonyls (*m/z* 44, 58, 72, and 86),
474 crotonaldehyde (*m/z* 70), hydroxyacetone (*m/z* 74) and the furan-
475 derivate C2-furan/furfural (*m/z* 96), furfuryl alcohol (*m/z* 98),
476 methyl-furfural (*m/z* 110) and hydroxymethylfurfural (*m/z* 126).
477 Lower factor loadings in PC2 occur for phenol-derivates guaiacol
478 (*m/z* 124), methyl-guaiacol (*m/z* 138), eugenol (*m/z* 164), catechol
479 (*m/z* 110) and coniferylalcohol/vinylsyringol (*m/z* 180). Furans,
480 carbonyls and phenolic species refer to specific decomposition
481 products of (hemi-)cellulose and lignin, therefore the positive load-
482 ing of PC2 can be regarded as primary decomposition. Conversely,
483 PC loadings in negative direction contain mainly unsaturated
484 hydrocarbons, such as propene (*m/z* 42), propyne/propadiene (*m/z*
485 40), butadiene (*m/z* 54), toluene (*m/z* 92), isoprene (*m/z* 68),

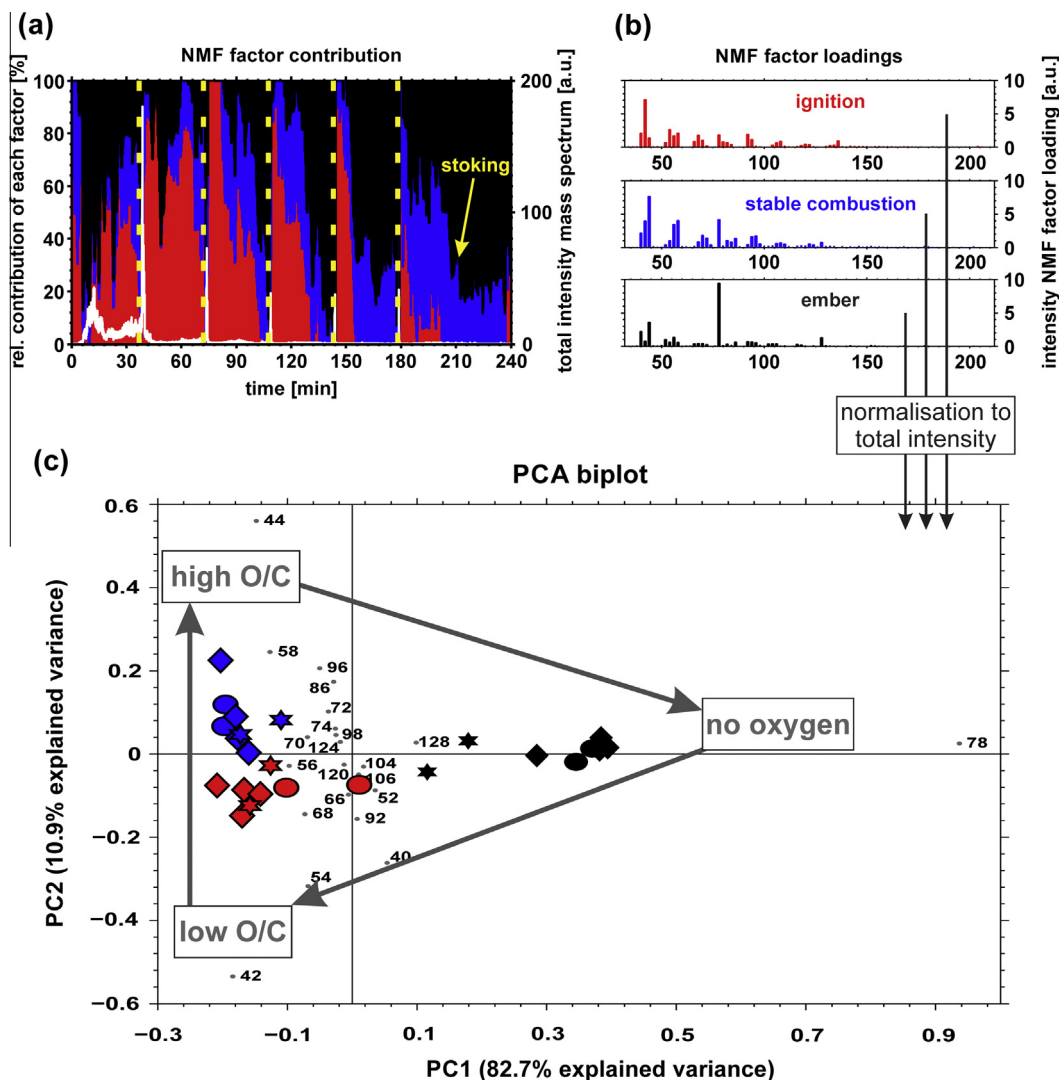


Fig. 3. (a) Relative NMF factor contribution representing burning phases ‘ignition’, ‘stable combustion’ and ‘ember’ and total intensity of original mass spectra (white). Batch limits are indicated by yellow dashed lines. (b) NMF factor loadings which can be regarded as mass spectrum for the respective burning phase. (c) PCA-biplot of the first two principal components (PC1 and PC1) for NMF factor loadings of ‘ignition’ (red), ‘stable combustion’ (blue) and ‘ember’ (black). Score coefficients for types of wood are marked with circles (beech), diamonds (birch) and hexagrams (spruce). Grey diamonds with numbers refer to m/z in PC loadings, which can be classified according to their estimated oxygen-to-carbon ratio O/C. For a better visualisation, only factor loadings >0.015 in at least one PC are illustrated. (For interpretation of the references to colour in this figure legend, the reader is referred to the web version of this article.)

486 cyclopentadiene (m/z 66), vinylacetylene (m/z 52), C_2 -benzene (m/z 106), styrene (m/z 104) and indane (m/z 118). Because of nominal mass resolution, m/z 68 and m/z 106 can also be allocated to furan and benzaldehyde. In contrast to positive PC2 loadings, these m/z do not constitute wood-specific combustion products and are most likely formed by secondary reactions such as water dissociation from hydroxyl groups through chemical elimination reactions or pyrosynthesis in flames. Therefore, even though generally highest emissions occur during the ignition of new logs, the ratio of primary to secondary decomposition products is lower for the burning phase ‘ignition’ compared to ‘stable combustion’. When the wood combustion turns through the formation of char into glowing embers, benzene formed by pyrosynthesis is the most prominent VOC by far.

499 Estimating the oxygen-to-carbon ratio O/C of detected m/z , the combustion progress might be monitored on-the-fly by SPI-TOFMS. All together, starting from ‘ember’ in the PCA score plot, burning phases are distributed clockwise towards an increasing O/C ratio and higher proportion of primary decomposition products on the organic emission.

4. Conclusion

506 This study investigated VOC to SVOC emissions from log wood combustion in a commercially available modern masonry heater burning three commonly types of firewood (beech, birch and spruce). Special focus was placed on the temporal trend of VOC and IVOC during the combustion process using the benefits of SPI-TOFMS. Some hazardous VOC, such as butadiene or styrene, could be semi-quantified. Updated emission factors (EF) for state-of-the-art wood stoves are important to feed atmospheric models for calculations of emission inventories and prediction of future scenarios. If air staging becomes more established in the future, the local atmosphere of areas with much residential wood combustion will change, so atmospheric metrics such as the ratio of toluene to benzene would have to be reconsidered.

507 Combustion conditions play a more important role for the emissions: Especially the ignition of the first batch is crucial, which has been demonstrated by a detailed comparison of the experiments ‘spruce1’ and ‘spruce2’. Organic emissions increase dramatically if the temperature drops during the ignition before the stable burn-

ing phase has been reached. In particular, primary decomposition products from lignin or carbohydrates were more enhanced than unsaturated hydrocarbons from secondary decomposition and pyrosynthesis. In general, intensities of all m/z in the first two batches represented more than 50% of the total intensity of the respective m/z from six consecutive batches; even 55–66% of benzene in the exhaust gas was released during the first batch solely. This shows that the development needs regarding the organic emissions from modern masonry heaters are particularly in controlling combustion efficiency during ignition and in the first wood batches.

Additionally, the molecular signature of burning phases was determined by non-negative matrix factorisation (NMF) and more detailed examined by principal component analysis (PCA). This enables to monitor burning phases on-the-fly by the ratio of primary decomposition products from lignin and (hemi-)cellulose to secondary decomposition or pyrosynthetic products for a better understanding of the wood combustion process.

Compared to previous studies with masonry heaters without air staging, the amount of organic emissions dropped significantly. However, toxicological studies must follow, for example by exposure of wood combustion aerosol to lung cells in an air-liquid-interface (ALI) [45,46] to reveal synergistic effects and enable a full assessment of improvements in stove construction.

Conflict of interest

The authors declare that they have no conflict of interest.

Acknowledgements

This work was carried out at the University of Eastern Finland, Department of Environmental Science in cooperation with Helmholtz Virtual Institute of Complex Molecular Systems in Environmental Health (HICE), funded by The Helmholtz Impulse and networking Funds of the Helmholtz Association (Germany, HICE), the Academy of Finland (grants 259946 and 258315) and the University of Eastern Finland for the project “sustainable bioenergy, climate change and health”. Furthermore, the authors would like to acknowledge Dr. Martin Sklorz and Christopher P. R uger for their suggestions and critical comments.

Appendix A. Supplementary material

Supplementary data associated with this article can be found, in the online version, at <http://dx.doi.org/10.1016/j.fuel.2016.03.036>.

References

- [1] Eurostat. Production and consumption of wood in the EU27. Statistical Office of the European Communities Eurostat; 2012.
- [2] Gaeggeler K, Pr ev ot ASH, Dommen J, Legreid G, Reimann S, Baltensperger U. Residential wood burning in an Alpine valley as a source for oxygenated volatile organic compounds, hydrocarbons and organic acids. *Atmos Environ* 2008;42:8278–87.
- [3] Genberg J, Denier Van Der Gon HAC, Simpson D, Swietlicki E, Areskoug H, Beddows D, et al. Light-absorbing carbon in Europe – measurement and modelling, with a focus on residential wood combustion emissions. *Atmos Chem Phys* 2013;13:8719–38.
- [4] Salthammer T, Schripp T, Wientzek S, Wensing M. Impact of operating wood-burning fireplace ovens on indoor air quality. *Chemosphere* 2014;103:205–11.
- [5] B olling AK, Totlandsdal AI, Sallsten G, Braun A, Westerholm R, Bergvall C, et al. Wood smoke particles from different combustion phases induce similar pro-inflammatory effects in a co-culture of monocyte and pneumocyte cell lines. *Part Fibre Toxicol* 2012;9.
- [6] Totlandsdal AI,  vrevik J, Cochran RE, Herseth JI, B olling AK, L ag M, et al. The occurrence of polycyclic aromatic hydrocarbons and their derivatives and the proinflammatory potential of fractionated extracts of diesel exhaust and wood smoke particles. *J Environ Sci Health – Part A Toxic/Hazard Substances Environ Eng* 2014;49:383–96.

- [7] Uski O, Jalava PI, Happonen MS, Leskinen J, Sippula O, Tissari J, et al. Different toxic mechanisms are activated by emission PM depending on combustion efficiency. *Atmos Environ* 2014;89:623–32.
- [8] Sciare J, Oikonomou K, Favez O, Liakakou E, Markaki Z, Cachier H, et al. Long-term measurements of carbonaceous aerosols in the Eastern Mediterranean: evidence of long-range transport of biomass burning. *Atmos Chem Phys* 2008;8:5551–63.
- [9] Kowal EA, Seneviratne U, Wickramaratne S, Doherty KE, Cao X, Tretyakova N, et al. Structures of exocyclic R, R-and S, S-N6, N 6-(2,3-dihydroxybutan-1,4-diyl)-2'-deoxyadenosine adducts induced by 1,2,3,4-diepoxybutane. *Chem Res Toxicol* 2014;27:805–17.
- [10] Whysner J, Reddy MV, Ross PM, Mohan M, Lax EA. Genotoxicity of benzene and its metabolites. *Mutat Res – Rev Mutat Res* 2004;566:99–130.
- [11] Evtugina M, Alves C, Calvo A, Nunes T, Tarelho L, Duarte M, et al. VOC emissions from residential combustion of Southern and mid-European woods. *Atmos Environ* 2014;83:90–8.
- [12] Lingens A, Windeisen E, Wegener G. Investigating the combustion behaviour of various wood species via their fire gases. *Wood Sci Technol* 2005;39:49–60.
- [13] McDonald JD, Zielinska B, Fujita EM, Sagebiel JC, Chow JC, Watson JG. Fine particle and gaseous emission rates from residential wood combustion. *Environ Sci Technol* 2000;34:2080–91.
- [14] Johansson LS, Leckner B, Gustavsson L, Cooper D, Tullin C, Potter A. Emission characteristics of modern and old-type residential boilers fired with wood logs and wood pellets. *Atmos Environ* 2004;38:4183–95.
- [15] Brilli F, Gioli B, Ciccioli P, Zona D, Loreto F, Janssens IA, et al. Proton Transfer Reaction Time-of-Flight Mass Spectrometry (PTR-TOF-MS) determination of volatile organic compounds (VOCs) emitted from a biomass fire developed under stable nocturnal conditions. *Atmos Environ* 2014;97:54–67.
- [16] Fitzpatrick EM, Ross AB, Bates J, Andrews G, Jones JM, Phylaktou H, et al. Emission of oxygenated species from the combustion of pine wood and its relation to soot formation. *Process Saf Environ Prot* 2007;85:430–40.
- [17] Christian TJ, Yokelson RJ, Carvalho Jr JA, Griffith DWT, Alvarado EC, Santos JC, et al. The tropical forest and fire emissions experiment: Trace gases emitted by smoldering logs and dung from deforestation and pasture fires in Brazil. *J Geophys Res: Atmos* 2007;112.
- [18] Yokelson RJ, Burling IR, Gilman JB, Warneke C, Stockwell CE, De Gouw J, et al. Coupling field and laboratory measurements to estimate the emission factors of identified and unidentified trace gases for prescribed fires. *Atmos Chem Phys* 2013;13:89–116.
- [19] Streibel T, M uhlberger F, Gei sler R, Saraji-Bozorgzad M, Adam T, Zimmermann R. Influence of sulphur addition on emissions of polycyclic aromatic hydrocarbons during biomass combustion. *Proc Combust Inst* 2014.
- [20] Elsasser M, Busch C, Orasche J, Sch on C, Hartmann H, Schnelle-Kreis J, et al. Dynamic changes of the aerosol composition and concentration during different burning phases of wood combustion. *Energy Fuels* 2013;27:4959–68.
- [21] Gullett B, Touati A, Oudejans L. Use of REMPI-TOFMS for real-time measurement of trace aromatics during operation of aircraft ground equipment. *Atmos Environ* 2008;42:2117–28.
- [22] Greenberg JP, Friedli H, Guenther AB, Hanson D, Harley P, Karl T. Volatile organic emissions from the distillation and pyrolysis of vegetation. *Atmos Chem Phys* 2006;6:81–91.
- [23] Streibel T, Gei sler R, Saraji-Bozorgzad M, Sklorz M, Kaisersberger E, Denner T, et al. Evolved gas analysis (EGA) in TG and DSC with single photon ionisation mass spectrometry (SPI-MS): molecular organic signatures from pyrolysis of soft and hard wood, coal, crude oil and ABS polymer. *J Therm Anal Calorim* 2009;96:795–804.
- [24] Yang H, Yan R, Chen H, Lee DH, Zheng C. Characteristics of hemicellulose, cellulose and lignin pyrolysis. *Fuel* 2007;86:1781–8.
- [25] Nuutinen K, Jokiniemi J, Sippula O, Lamberg H, Sutinen J, Horttanainen P, et al. Effect of air staging on fine particle, dust and gaseous emissions from masonry heaters. *Biomass Bioenergy* 2014;67:167–78.
- [26] Ferge T, Maguhn J, Hafner K, M uhlberger F, Davidovic M, Warnecke R, et al. On-line analysis of gas-phase composition in the combustion chamber and particle emission characteristics during combustion of wood and waste in a small batch reactor. *Environ Sci Technol* 2005;39:1393–402.
- [27] Fendt A, Streibel T, Sklorz M, Richter D, Dahmen N, Zimmermann R. On-line process analysis of biomass flash pyrolysis gases enabled by soft photoionization mass spectrometry. *Energy Fuels* 2012;26:701–11.
- [28] Hansen N, Cool TA, Westmoreland PR, Kohse-H oinghaus K. Recent contributions of flame-sampling molecular-beam mass spectrometry to a fundamental understanding of combustion chemistry. *Prog Energy Combust Sci* 2009;35:168–91.
- [29] Reda AA, Czech H, Schnelle-Kreis J, Sippula O, Orasche J, Weggler B, et al. Analysis of gas phase carbonyl compounds in emissions from modern wood combustion appliances: influence of wood type and combustion appliance. *Energy Fuels* 2015;29:3897–907.
- [30] Adam T, Zimmermann R. Determination of single photon ionization cross sections for quantitative analysis of complex organic mixtures. *Anal Bioanal Chem* 2007;389:1941–51.
- [31] Berry MW, Browne M, Langville AN, Pauca VP, Plemmons RJ. Algorithms and applications for approximate nonnegative matrix factorization. *Comput Stat Data Anal* 2007;52:155–73.
- [32] Paatero P, Tapper U. Positive matrix factorization: a non-negative factor model with optimal utilization of error estimates of data values. *Environmetrics* 1994;5:111–26.

587
588
589
590
591
592
593
594
595
596
597
598
599
600
601
602
603
604
605
606
607
608
609
610
611
612
613
614
615
616
617
618
619
620
621
622
623
624
625
626
627
628
629
630
631
632
633
634
635
636
637
638
639
640
641
642
643
644
645
646
647
648
649
650
651
652
653
654
655
656
657
658
659
660
661
662
663
664
665
666
667
668
669
670
671

- 672 [33] Lamberg H, Nuutinen K, Tissari J, Ruusunen J, Yli-Pirilä P, Sippula O, et al. Physicochemical characterization of fine particles from small-scale wood
673 combustion. *Atmos Environ* 2011;45:7635–43. 694
- 674 [34] Tissari J, Hytönen K, Sippula O, Jokiniemi J. The effects of operating conditions
675 on emissions from masonry heaters and sauna stoves. *Biomass Bioenergy*
676 2009;33:513–20. 695
- 677 [35] Tissari J, Lyyränen J, Hytönen K, Sippula O, Tapper U, Frey A, et al. Fine particle
678 and gaseous emissions from normal and smouldering wood combustion in a
679 conventional masonry heater. *Atmos Environ* 2008;42:7862–73. 696
- 680 [36] Massart DL, Vandeginste BGM, Buydens LMC, de Jong S, Lewi PJ, Smeyers-
681 Verbeke J. *Handbook of chemometrics and qualimetrics: Part A*. first
682 ed. Amsterdam: Elsevier Science B. V.; 1997. p. 112f. 697
- 683 [37] Ledesma EB, Campos C, Cranmer DJ, Foytik BL, Ton MN, Dixon EA, et al. Vapor-
684 phase cracking of eugenol: distribution of tar products as functions of
685 temperature and residence time. *Energy Fuels* 2013;27:868–78. 698
- 686 [38] Nowakowska M, Herbinet O, Dufour A, Glaude PA. Detailed kinetic study of
687 anisole pyrolysis and oxidation to understand tar formation during biomass
688 combustion and gasification. *Combust Flame* 2013. 699
- 689 [39] N. Hansen, J.A. Miller, T. Kasper, K. Kohse-Höinghaus, P.R. Westmoreland, J.
690 Wang, T.A. Cool, Benzene formation in premixed fuel-rich 1,3-butadiene
691 flames C3 – Proceedings of the Combustion Institute. In: 32nd international
692 symposium on combustion, vol. 32(1); 2009. p. 623–30. 700
- [40] Li W, Law ME, Westmoreland PR, Kasper T, Hansen N, Kohse-Höinghaus K. Multiple benzene-formation paths in a fuel-rich cyclohexane flame. *Combust Flame* 2011;158:2077–89. 694
- [41] Shen DK, Gu S. The mechanism for thermal decomposition of cellulose and its main products. *Bioresour Technol* 2009;100:6496–504. 695
- [42] Richter H, Howard JB. Formation of polycyclic aromatic hydrocarbons and their growth to soot—a review of chemical reaction pathways. *Prog Energy Combust Sci* 2000;26:565–608. 696
- [43] Jordan C, Fitz E, Hagan T, Sive B, Frinak E, Haase K, et al. Long-term study of VOCs measured with PTR-MS at a rural site in New Hampshire with urban influences. *Atmos Chem Phys* 2009;9:4677–97. 697
- [44] Trendafilov NT. From simple structure to sparse components: a review. *Comput Statistics* 2014;29:431–54. 698
- [45] Paur HR, Cassee FR, Teeguarden J, Fissan H, Diabate S, Aufderheide M, et al. In-vitro cell exposure studies for the assessment of nanoparticle toxicity in the lung – a dialog between aerosol science and biology. *J Aerosol Sci* 2011;42:668–92. 699
- [46] Oeder S, Kanashova T, Sippula O, Sapcariu SC, Streibel T, Arteaga-Salas JM, et al. Particulate matter from both heavy fuel oil and diesel fuel shipping emissions show strong biological effects on human lung cells at realistic and comparable in vitro exposure conditions. *PLoS ONE* 2015;10:1932–6203. 700

UNCORRECTED PROOF